From populations to networks: Relating diversity indices and frustration in signed graphs

PNAS Nexus, 2024, 3, 1–11
https://doi.org/10.1093/pnasnexus/pgae046
Advance access publication 3 February 2024
Research Report

From populations to networks: Relating diversity indices and frustration in signed graphs

Angela Fontan [a], Marco Ratta [b] and Claudio Altafini [c,*]

[a]Division of Decision and Control Systems, School of Electrical Engineering and Computer Science, KTH Royal Institute of Technology, Stockholm SE-100 44, Sweden
[b]Department of Mathematical Sciences "G.L. Lagrange", Politecnico di Torino, Turin 10129, Italy
[c]Division of Automatic Control, Department of Electrical Engineering, Linköping University, Linköping SE-58183, Sweden
*To whom correspondence should be addressed: Email: claudio.altafini@liu.se
Edited By: Alberto Guadagnini

Abstract

Diversity indices of quadratic type, such as fractionalization and Simpson index, are measures of heterogeneity in a population. Even though they are univariate, they have an intrinsic bivariate interpretation as encounters among the elements of the population. In the paper, it is shown that this leads naturally to associate populations to weakly balanced signed networks. In particular, the frustration of such signed networks is shown to be related to fractionalization by a closed-form expression. This expression allows to simplify drastically the calculation of frustration for weakly balanced signed graphs.

Keywords: complex networks, frustration, fractionalization, signed graphs, diversity indices in population

Significance Statement

The paper shows that quadratic diversity indices, commonly used to quantify heterogeneity in a population, have an intrinsic network interpretation, provided we consider signed graphs, i.e. graphs in which positive edges represent the probability of within-group encounters and negative edges that of between-groups encounters. Furthermore, these diversity indices are shown to be related by closed-form expression to a classical measure of unbalance in signed graphs, the so-called frustration.

Introduction

Diversity indices are univariate measures of fragmentation in a population, and allow to quantify the relative importance of the groups (representing, depending on the context, subpopulations, species, types, samples, etc.) that compose the population (1–3). They have been widely used for several decades and in many different domains, from Ecology (4) to Sociology (5), from Biology (6) to Economics (7), from Demography (8) to Political Sciences (9), etc.

A commonly used diversity index is the so-called fractionalization index (10). For a population of n elements subdivided into q groups of cardinality $c_1, \ldots, c_q$, fractionalization is defined as

$$F = 1 - \frac{\sum_{i=1}^{q} c_i^2}{n^2}. \tag{1}$$

The fractionalization F corresponds to the probability that two randomly drawn elements from the population are not from the same group. F is also known as the Gini–Simpson index in Ecology (11), the Blau index (12), or the Gibbs–Martin index (13) in Sociology, Psychology, and Management Sciences. F can vary between 0 and $1-\frac{1}{n}$, corresponding, respectively, to a population composed of a single group and to a population composed of n groups of size 1.

Associated to F one can consider a measure of "effective" number of groups

$$E = \frac{n^2}{\sum_{i=1}^{q} c_i^2} = \frac{1}{1-F}, \tag{2}$$

which is known in Political Sciences as the Laakso–Taagepera effective number of parties (9), and in Ecology as the inverse Simpson index—the Simpson index being defined as $H = \sum_{i=1}^{q} \left(\frac{c_i}{n}\right)^2 = \frac{1}{E}$ (11). H is also known in Economics as the Herfindahl–Hirschman index (14), where the fractions of unit $\frac{c_i}{n}$ represent e.g. size of firms in an industrial sector or market shares of a certain product. In particular, H is frequently applied by legislators in competition law and antitrust regulation as a measure of market concentration in industrial sectors (15).

All the indices mentioned so far are univariate, i.e. they group the population along a single dimension, and are of quadratic type. The interpretation of F and H as probability of (pairwise) encounters suggests that quadratic diversity indices can be considered bivariate quantities, and associated to networks of

Competing Interest: The authors declare no competing interest.
Received: August 28, 2023. **Accepted:** January 22, 2024

interactions among the entities forming the population. In fact, whenever a population can be split into q groups according to some classification dimension, then the n entities of the population can be represented as the nodes of a graph partitioned into q communities, and their encounters as the edges of the graph. Scope of this paper is to make this association precise and to provide a network interpretation of the diversity indices.

In particular, if F represents the probability of interspecific (i.e. between-groups) encounters and is an index of diversity, $H = 1 - F$ can be understood as probability of intraspecific (i.e. within-group) encounters and is a concentration index. In order to represent both between-groups and within-group interactions on a graph, we need two qualitatively different types of edges. A natural choice is to consider signed (undirected) graphs, and to associate positive edges to within-group interactions and negative edges to between-groups interactions. In other words, positive edges represent some form of similarity in a classification, for instance, in the examples we present below, same political party or same ethnolinguistic group, while negative edges represent diversity in the same classification, e.g. different parties or ethnolinguistic groups.

A key contribution of this paper is to show that the diversity indices mentioned above (in particular fractionalization and effective number of groups) can be linked to well-established tools used to investigate signed graphs, like the notion of frustration from structural balance theory. Structural balance theory has been used for several decades in various fields ranging from Sociology (16) to Statistical Physics (17), from Biology (18) to Engineering (19). Two concepts frequently used in this theory to investigate the properties of signed graphs are strong and weak structural balance (hereafter, for short, strong and weak balance) (20–22). These two concepts can be easily captured by looking at a triad of nodes, see Fig. 1A. A strongly balanced triad corresponds to a triangle graph with an even number of negative edges, while weak balance corresponds to a triangle not having exactly one negative edge (23). The two characterizations are not equivalent: a strongly balanced graph is also weakly balanced but not vice versa. This is true also for general graphs of n nodes: strong balance corresponds to the existence of a partition of the nodes in two disjoint factions, such that all within-faction edges are positive and all between-factions edges negative. Weak balance corresponds instead to the existence of two or more groups (or communities) of nodes such that all edges within a group are positive and all edges between groups are negative, see Fig. 1B. By construction, the signed graph associated to a population subdivided into q groups is weakly balanced.

In this paper, we consider such population-based weakly balanced signed graphs and study their frustration (denoted ζ below), i.e. their "distance to strong balance" (16, 24, 25), a common measure of disorder of a signed graph, applicable also to the weakly balanced case (25). In particular, we obtain that when the edge distribution in the signed graph is uniform (i.e. when the connectivity of the graph follows an Erdös–Rényi model), the frustration has the interpretation of "best bipartition," i.e. splitting of the q groups of the population into two disjoint factions having size (measured as sum of the cardinalities of the groups) which is as equal as possible. Such best bipartition is shown to always respect the group structure, meaning that computing frustration becomes a problem of group partitioning, which significantly simplifies its calculation. Furthermore, it is shown in the paper that the value of frustration ζ is related to the fractionalization F by a closed-form expression, depending on the node excess in the aforementioned best bipartition of the groups. An analysis of the properties associated to the relationship between ζ and F is carried out when the group sizes of the population are drawn from uniform and power-law distributions. The tools developed in the paper are then applied to various datasets drawn from Political Sciences, Demography, and Economics.

Results

Frustration for weakly balanced signed graphs

For graphs that are not balanced, various measures of the "distance to strong balance" (or graph unbalance) have been proposed in the literature (25–30). In particular, a commonly used metric for strong balance is the frustration index (the name comes from spin glass theory (17, 26), and it is sometimes also called line index of balance (31)), here defined as the least fraction of the total number of edges that must change sign in order to attain strong balance. For a signed graph of n nodes, if A is the signed adjacency matrix (of entries A_{ij} equal to ± 1 or 0), and we associate to the nodes a vector s of "spin" variables $s_i = \pm 1$, then the frustration ζ is the minimum over all possible spin assignments of the relative energy functional $e(s)$:

$$\zeta = \min_{s_i, s_j \in \pm 1} e(s) = \min_{s_i, s_j \in \pm 1} \frac{1}{2m} \sum_{(i,j) \in \mathcal{E}} (1 - A_{ij} s_i s_i), \tag{3}$$

where $\mathcal{E}$ is the set of edges of the graph and m is the total (expected) number of edges in the graph, see Methods for more details and Table S1 for a summary of notations. Computing ζ is an NP-hard problem (equivalent to solving a MAX-CUT problem (32)). For weak balance, the problem is more complicated, as the groups of nodes must first be identified. If the groups are given in advance, as we assume here, then frustration is still a suitable measure of unbalance (25).

A first result of the paper is that for weakly balanced signed graphs in which all edges are equiprobable (i.e. when the topology follows a Erdös–Rényi model), denoting $\mathcal{F}^+_{\text{best}}$ and $\mathcal{F}^-_{\text{best}}$ the two factions ("spin-up" and "spin-down") in the "ground state" of Eq. 3, then the $\{\mathcal{F}^+_{\text{best}}, \mathcal{F}^-_{\text{best}}\}$ optimal partition always respects the group structure, i.e. a group is never split into two parts when computing the optimal spin configuration s that minimizes $e(s)$. Such coarse-graining of the ground state spin assignment drastically simplifies the calculation of the frustration: computing ζ amounts to partitioning the groups into two factions of size which is as equal as possible given the group sizes $c_1, \ldots, c_q$. Letting $n_{\mathcal{F}^+}$ and $n_{\mathcal{F}^-}$ be the size of a partition $\{\mathcal{F}^+, \mathcal{F}^-\}$ of the nodes, computing ζ corresponds then to solving

$$\max_{\mathcal{F}^+} \left(n_{\mathcal{F}^+} (n - n_{\mathcal{F}^+}) \right), \tag{4}$$

where the max is over all possible bipartitions of the integers $c_1, \ldots, c_q$. Theorem 1 in the supplementary material provides a technical proof of these statements.

Connecting frustration and fractionalization on weakly balanced graphs

As mentioned, on a graph, diversity with respect to the classification dimension can be captured by the edge signature: adjacent nodes coparticipating in the same group are linked by positive edges, while adjacent nodes belonging to different groups are linked by negative edges. The resulting graph is therefore a weakly balanced signed graph by construction. A second result of the paper is that when the connectivity of the graph follows an Erdös–Rényi model, it is possible to obtain a

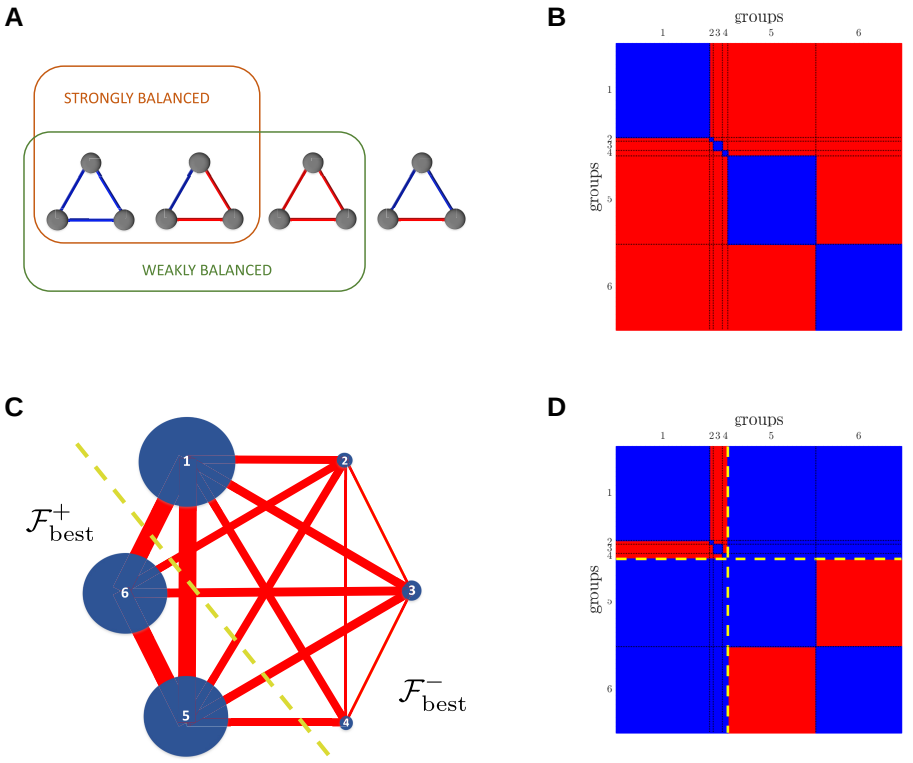

Fig. 1. Strongly and weakly balanced signed graphs. A) Strong and weak balance in terms of elementary triplets. A triplet is strongly balanced if it contains an even number of negative edges, and weakly balanced if it does not contain exactly one negative edge. B) Example of weakly balanced graph of size $n = 1{,}000$ with 6 groups, of size $c_i = 326, 13, 32, 19, 311, 299$. The panel shows the corresponding adjacency matrix A (in blue: positive edges; in red: negative edges). C) Each group can be condensed into a single node in the matrix W (see Methods), with edge weights between groups i and j becoming $W_{ij} = pc_ic_j$. In the panel, node size is proportional to c_i and edge width to c_ic_j. The optimal partition into two factions is $\mathcal{F}^+_{\text{best}} = \{5, 6\}$ and $\mathcal{F}^-_{\text{best}} = \{1, 2, 3, 4\}$ (dashed yellow line) and $\ell_{\text{best}} = 220$ (i.e. $r_{\text{best}} = 0.44$). D) What is shown is the adjacency matrix after an optimal "gauge transformation": when the spin variables in $\mathcal{F}^-_{\text{best}}$ and $\mathcal{F}^+_{\text{best}}$ are associated with -1 and $+1$, respectively, and placed on the diagonal of a matrix S, then in the gauge transformed adjacency matrix SAS the off-diagonal blocks change sign. The residual number of negative edges (normalized by the total number of edges) gives the frustration of the graph.

closed-form expression for the relationship between frustration ζ and fractionalization F:

$$\zeta = F - \frac{1}{2} + \frac{1}{2} r^2_{\text{best}}, \tag{5}$$

where the relative node excess r_{best} is expressed as $r_{\text{best}} = \frac{\ell_{\text{best}}}{n/2}$, with ℓ_{best} the least number of nodes in excess (with respect to an equal-cardinality splitting) among all possible ways to partition the q communities into two factions $\mathcal{F}^+$ and $\mathcal{F}^-$ (i.e. $\ell_{\text{best}} = n_{\mathcal{F}^+_{\text{best}}} - n/2$, if we take $n_{\mathcal{F}^+_{\text{best}}} \geq n_{\mathcal{F}^-_{\text{best}}}$), see Methods. From $F = 1 - \frac{1}{E}$, Eq. 5 can be reexpressed in terms of E as

$$\zeta = \frac{1}{2} - \frac{1}{E} + \frac{1}{2} r^2_{\text{best}}, \tag{6}$$

i.e. the frustration ζ and the effective number of parties E are inversely related. Since $r_{\text{best}} = n_{\mathcal{F}^+_{\text{best}}}/(n/2) - 1$, the practical meaning of Eq. 5 is that as soon as the number of groups is sufficiently high (and hence a 50–50% splitting becomes more likely to exist, implying $r_{\text{best}} \approx 0$) then frustration becomes essentially equal to fractionalization, up to the additive constant 1/2.

In order to explore the properties of the relationship in Eq. 5, we generated numerical examples of populations with different group size distributions, uniform (Fig. 2) and power-law (Fig. 3). In Fig. 2, weakly balanced signed Erdös–Rényi networks of size $n = 10^4$ with $q = 2, 3, \ldots, 20$ groups of randomly generated size c_i (such that $\sum_{i=1}^{q} c_i = n$) are produced and their fractionalization F, frustration ζ, and effective number of groups E are computed. As expected, both F and ζ grow with q. Furthermore, ζ and F become essentially identical (up to the 1/2 constant) as soon as $q \simeq 8$, see Fig. 2A. In other words, for q large enough, $\zeta = F - \frac{1}{2}$ is a valid approximation, meaning that F (an easily computable index) can be used to estimate ζ (which is NP-hard to compute even for weakly balanced Erdös–Rényi graphs). Deviations from this heuristic rule can occur only in two situations, detailed below, which essentially exhaust the spectrum of possibilities for which $r_{\text{best}} > 0$ and hence $\zeta \neq F - \frac{1}{2}$. The first and most important situation is when there exists a single group which is larger than $n/2$, and hence splitting into two factions, while respecting the partition into the groups necessarily leads to a node excess on the side of the largest group. In these cases, $r_{\text{best}} > 0$, see Fig. 2A. Most of these cases correspond to low fractionalization, since the presence of a large c_i renders the sum $\sum_i c_i^2/n^2$ close to 1. These cases also normally lead to low frustration, as the large block corresponding to the big c_i leaves little room for off-diagonal edges with negative signs. A second situation in which minor deviations between ζ and F can occur is when three large groups of approximately the same size exist (e.g. $\sim 30\%$ each). See the smaller bump for higher values of frustration and fractionalization in Fig. 2A. For instance, in the example of Fig. 1B, three similarly large groups make around 93% of the nodes, and the best bipartition has a node excess $\ell_{\text{best}} > 200$ out of

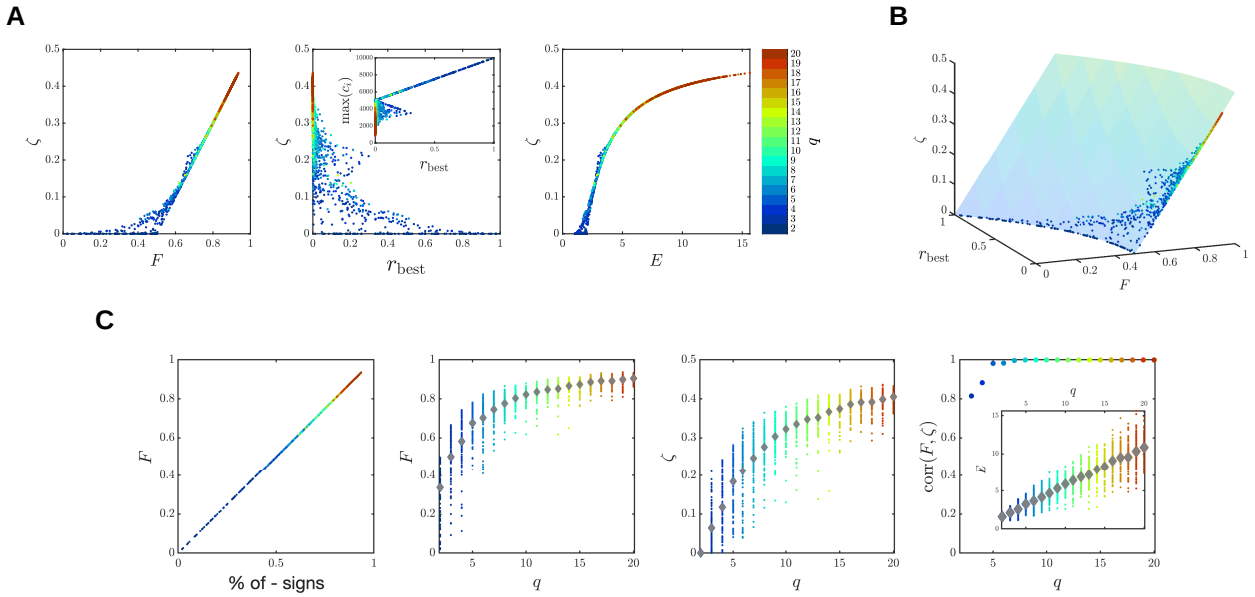

Fig. 2. Fractionalization vs. frustration in a weakly balanced network with group size distributed uniformly. Weakly balanced signed Erdös–Rényi networks of size $n = 10^4$ were generated containing $q = 2, \ldots, 20$ groups (100 instances for each q), see colorbar. A) Scatter plots of frustration ζ vs. fractionalization F, relative node excess r_{best}, and effective number of groups E. Inset in middle panel: r_{best} may be >0 even when each group has size $c_i < n/2$ (e.g. when there are three groups of similar size). B) 3D scatter plot of ζ, F, and r_{best}. C) Left panel: F is equal to the fraction of negative edges. Second and third panels: F and ζ both tend to grow with the number of groups q, and so does E (inset in the right panel). Right panel: the correlation between ζ and F approaches 1 when q grows.

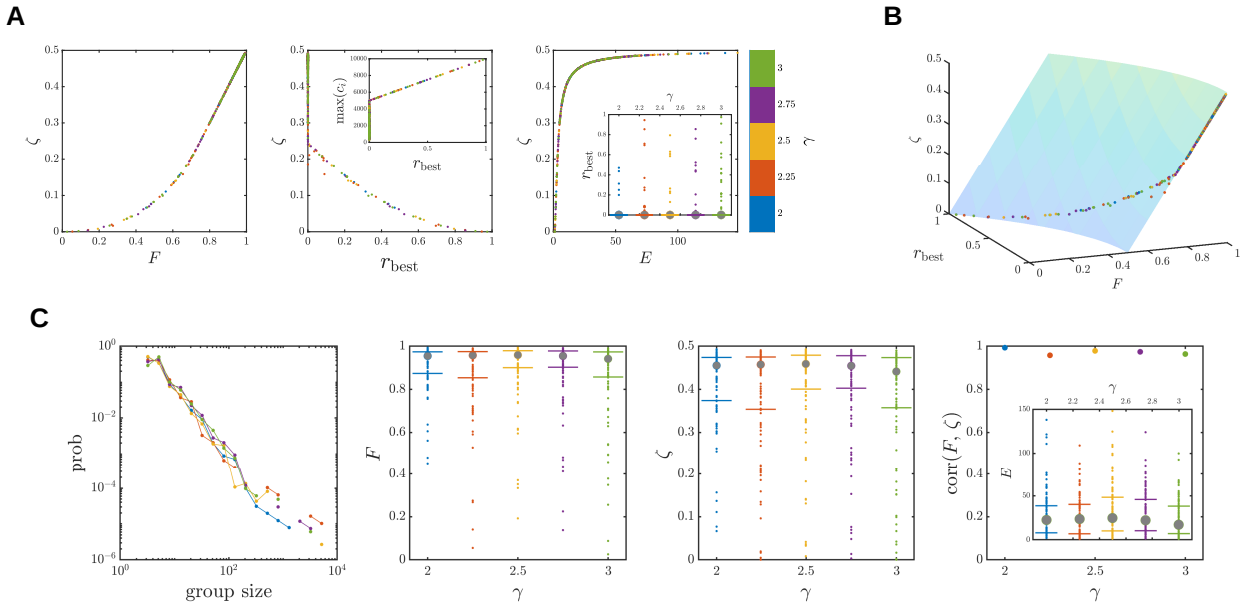

Fig. 3. Fractionalization vs. frustration in a weakly balanced network with groups size distributed according to a power-law. The exponent γ is chosen between 2 and 3, see colorbar. One hundred instances of size $n = 10^4$ are considered for each γ. A) Scatter plots of frustration ζ vs. fractionalization F, relative node excess r_{best}, and effective number of groups E. Inset in middle panel: r_{best} is >0 only when there is a group of size $c_i > n/2$. Notice how the relationship between ζ and F is now much more precise than in the uniform case: only one large component (exceeding 50% of the nodes) is present in basically all low frustration instances, regardless of the power exponent γ. In the inset in the right panel, median (circles) and quartiles (horizontal bars) of r_{best} are overlapping for all values of γ, meaning that the vast majority of samples has $r_{\text{best}} = 0$. B) 3D scatter plot of ζ, F, and r_{best}. C) Left panel: degree distribution of the group sizes c_i. Second and third panels: ζ and F as function of γ. Circles are medians and bars quartiles. No clear trend in γ is observed. Right panel: the correlation between ζ and F is >0.95.

$n = 1{,}000$ nodes. In this case, $\zeta = 0.43$ and $F = 0.71$. With the exclusion of the two aforementioned situations, we can conclude that on weakly balanced signed graphs the expression $\zeta = F - \frac{1}{2}$ can be used to avoid the NP-hard computation of the frustration ζ. Notice further in Fig. 2A how the dispersion existing in the frustration vs. fractionalization scatter plot gets significantly compressed when instead we look at frustration vs. effective number of groups. The price to pay for that compression is a

nonlinear dependence between ζ and E, as opposed to the linear dependence between ζ and F, see Eq. 6.

When instead the size c of the groups forming the population is drawn from a power-law distribution, $P(c) \sim c^{-\gamma}$, as in Fig. 3, then the presence of an abundant number of small groups favors the existence of an equal-cardinality bipartition, except when a large component exceeding 50% of the nodes is present. When this happens, $r_{\text{best}} > 0$, and the relationship between ζ and F tends to follow a curve which is nonlinear (see leftmost panel in Fig. 3A), but much more regular than for the uniform size case, as can be appreciated comparing the low ζ regions in Figs. 3A and 2A. In fact, in the power-law case, the correlation between ζ and F is >0.95 for all power-law exponents γ we consider. The case of three equally large groups essentially never appears for power-law generated group sizes, and basically all networks with low ζ correspond to cases in which $r_{\text{best}} > 0$. This determines the "rigid" relationship among ζ, F, and r_{best} seen in Fig. 3B.

Applications

We consider three different classes of real-world population datasets for which diversity indices are available, and compute the associated signed networks by putting each group in a network community characterized by internal positive edges and by negative edges connecting it with the other communities, so that the networks have the signed block structure shown in Fig. 1B. The edge probability is p ($0 < p \leq 1$) for the entire network, i.e. the networks have an Erdös–Rényi structure. This simple modeling choice is reasonable for a "no a priori information" setting, like when the only information available is the number and size of the groups (i.e. q and c_i, $i = 1, \ldots, q$).

Parliamentary networks

The first class of data corresponds to elected Members of Parliament (MPs) for 29 European countries over around four decades. The data were collected in Ref. (33) where they are described in more detail. Nodes are MPs and groups are political parties. For each country, after every general election, a new parliamentary network is produced. See Fig. S1 for the associated values of q (number of political parties) and Fig. S4 for the group size distribution.

Ethnolinguistic networks

The second class of data corresponds to fractions of population of a country according to the ethnolinguistic group they belong to. The data are taken from the Historical Index of Ethnic Fractionalization dataset (34). The dataset covers annually the period 1945–2013 for 165 countries across all continents. In this case, if nodes are individuals, n is in the order of millions. Under the assumption of random connectivity with equiprobable edges, it is convenient to map the population fractions into the weighted adjacency matrix W described in Eq. 7 of the Methods section, which condensates each ethnolinguistic group into a single node, and whose edge weights are proportional to the products of the population fractions of the two incident nodes of each edge. A matrix W is produced per country and per year. The number of groups in these matrices is given in Fig. S2, while the group size distribution is given in Figs. S5–S10.

Market shares of smartphone brands

Market shares of smartphone sales for the main manufacturers were downloaded from https://gs.statcounter.com/vendor-market-share for 22 countries in the years between 2015 and 2022. Similarly to the previous case, for each country a network is built by letting each brand be a node and connecting each node to any other node with a weight representing the product of the market fractions of the two brands incident to the edge. In this way, a weighted adjacency matrix W described in Eq. 7 is obtained for each year and for each country. The number of brands is given in Fig. S3 and the associated marker shares in Fig. S11.

Analysis

The analysis of the parliamentary networks shows, as expected for multiparty democracies, that the situation by far most common is a system in which no single party is above 50% of the seats. Consequently, the most common regime for our measures is the one in which $\zeta \approx F - \frac{1}{2}$, see Fig. 4A, with only minor exceptions for some legislatures in countries like Albania, North Macedonia, Serbia, and UK, see the details in Fig. S12. In fact, the correlation between ζ and F is on average 0.99, see rightmost panel in Fig. 4A. The same regime is followed by the market shares data, which also show an average correlation between ζ and F of 0.99, see Fig. 4C. Also in this case, the high fragmentation of the market (contended among many different companies) leads to a small ℓ_{best}. The only exception is Japan, where in fact the market is dominated by Apple with more than 65% of sold devices every year, see Fig. S13. The situation is somewhat different for the ethnolinguistic networks, where many states have homogeneous population or at least a large majority from a single ethnolinguistic group. This is true especially for the European countries, less for African countries, see details in Figs. S14–S19 and also the time evolution of frustration in Fig. 5. Ethnolinguistic homogeneity obviously translates into group size distribution which is markedly of power-law type, see Figs. S5–S10. From Fig. 4B, the correlation between ζ and F is still around 1 for most countries, with a few exceptions such as Algeria, El Salvador, Mauritius, Syria, and Thailand, all countries which are characterized by the presence of a large majoritarian ethnolinguistic group and two more minorities which impact in opposite ways the changes (over time) in ζ and F.

Time evolution of frustration

The time course of frustration for the three classes of empirical signed networks is shown in Fig. 5. What can be seen is that the frustration in the parliamentary networks is tendentially growing in the four decades of elections we monitor. This effect is analyzed and circumstantiated more in detail in Ref. (33), and reflects the increased fragmentation (i.e. F increases) of the political arena, with the collapse of the traditional ideological parties of the last century and the rise of different forces in many European countries, from green parties to protest movements, from nationalistic to populistic parties.

The trend toward increased fragmentation and therefore toward increased frustration in the associated signed networks appears to some extent also in the ethnolinguistic networks, although not for all continents. While in Asia, America, and Europe frustration seems to be growing, the opposite trend is observed in Africa. Notice that the starting point for many African nations (which is temporally located around 1960 in our dataset) is at a much higher frustration level than for the other continents, reflecting the way many African states were created, as postcolonian entities rather than as homogeneous ethnolinguistic groups. This is visible also on the group size distributions, which are often deviating from a power law, see Figs. S5 and S6. In this respect, European countries lie at the other end of the spectrum and for

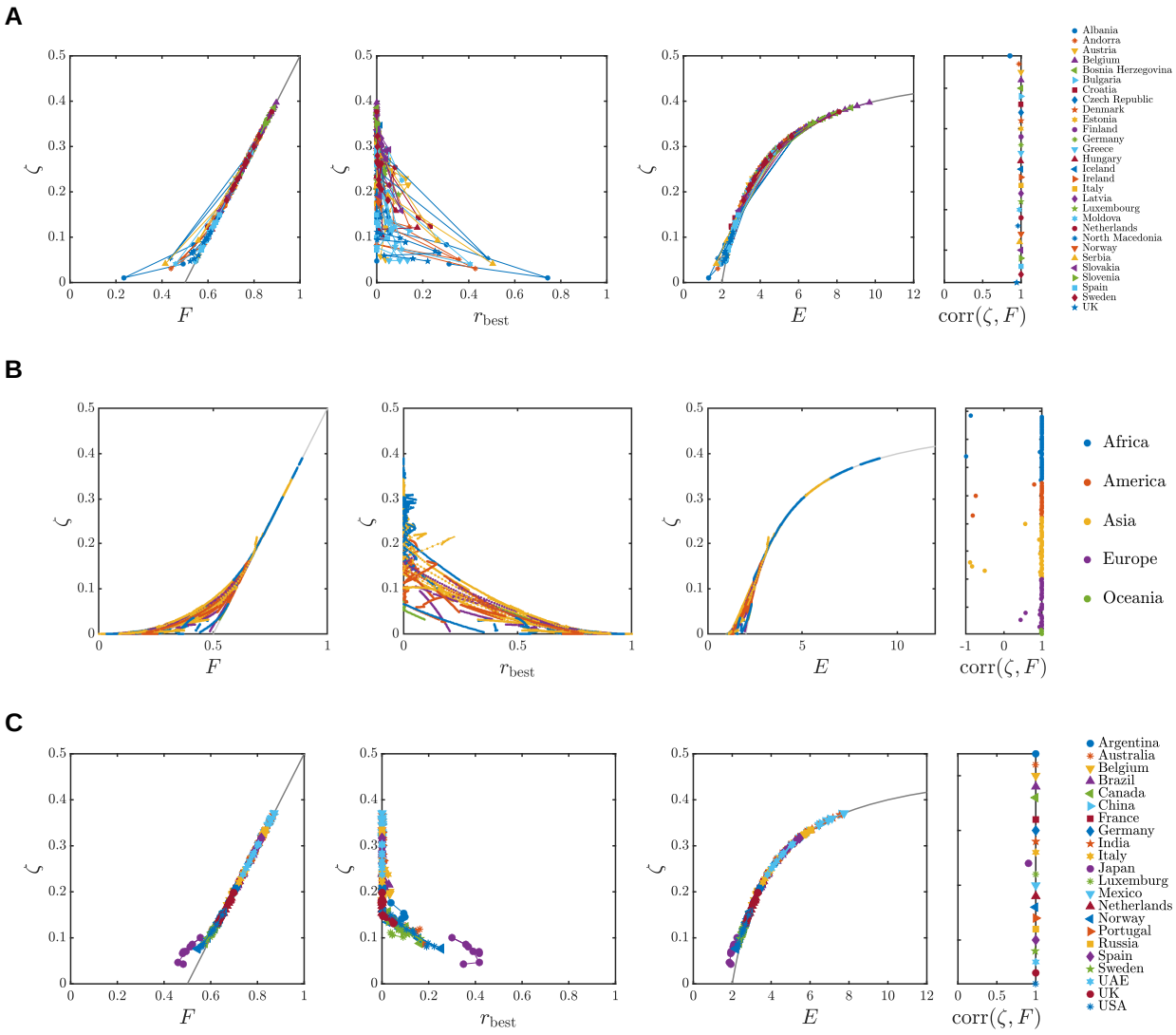

Fig. 4. Frustration and fractionalization in various applications. A) Parliamentary networks. B) Ethnolinguistic networks. C) Smartphone market shares. In each subfigure, the scatter plots of ζ vs. F, r_{best}, and E are shown in the three main panels, and the correlation between ζ and F in the right panel. Each country is represented by a different marker/color. The lines connect points that are consecutive in time for each country. The gray lines correspond to $\zeta = F - \frac{1}{2}$ and $\zeta = \frac{1}{2} - \frac{1}{E}$ (i.e. $r_{\text{best}} = 0$).

them (as for Asian and American countries, see Figs. S6–S10) the increase of frustration is likely a consequence of recent migratory movements and of globalization. Notice the opposite trend followed by most of the newly formed states emerged after the dissolution of Yugoslavia and Soviet Union in the nineties.

Discussion

Quantifying diversity in heterogeneous populations has been an important issue for several decades in a number of fields. While there exists a broad range of proposed measures (1, 2, 6), the quadratic indices considered in this paper are among the most popular in basically all fields. One of the reasons behind their widespread use is the (explicit or implicit) interpretation that can be given to quadratic indices as "encounters" among entities (or individuals, species, instances, etc.) of the different groups forming the population. Under the assumption of uniformity of such encounters, this interpretation leads naturally to constructing networks of interactions. Equally naturally, such networks must be signed, as signs are the simplest way to represent the two classes of interactions that characterize groups in a population: within-group and between-groups. The signed networks representation is by construction weakly balanced, with the groups that form the population appearing as communities in the network. Such modeling process seems all very straightforward and allows to build network interpretations of the quadratic diversity indices. For instance, the Simpson index H is often considered a weighted arithmetic mean of the proportional abundances $\frac{c_i}{n}$, where the weights are the proportional abundances $\frac{c_i}{n}$ themselves (1). The rationale behind this interpretation is that larger groups should be given larger representation when their importance is summarized into a scalar measure, a phenomenon called "class-size paradox" in Refs. (35, 36).[a] While this "size-biased sampling" phenomenon is a reasonable effect accepted in statistics, the choice of weights equal to the proportional abundances $\frac{c_i}{n}$ is just a convenient way to avoid arbitrary weights. In our network interpretation, instead, within-group encounters are *intrinsically* given by squared proportional abundances. In particular, since the number of edges[b] is

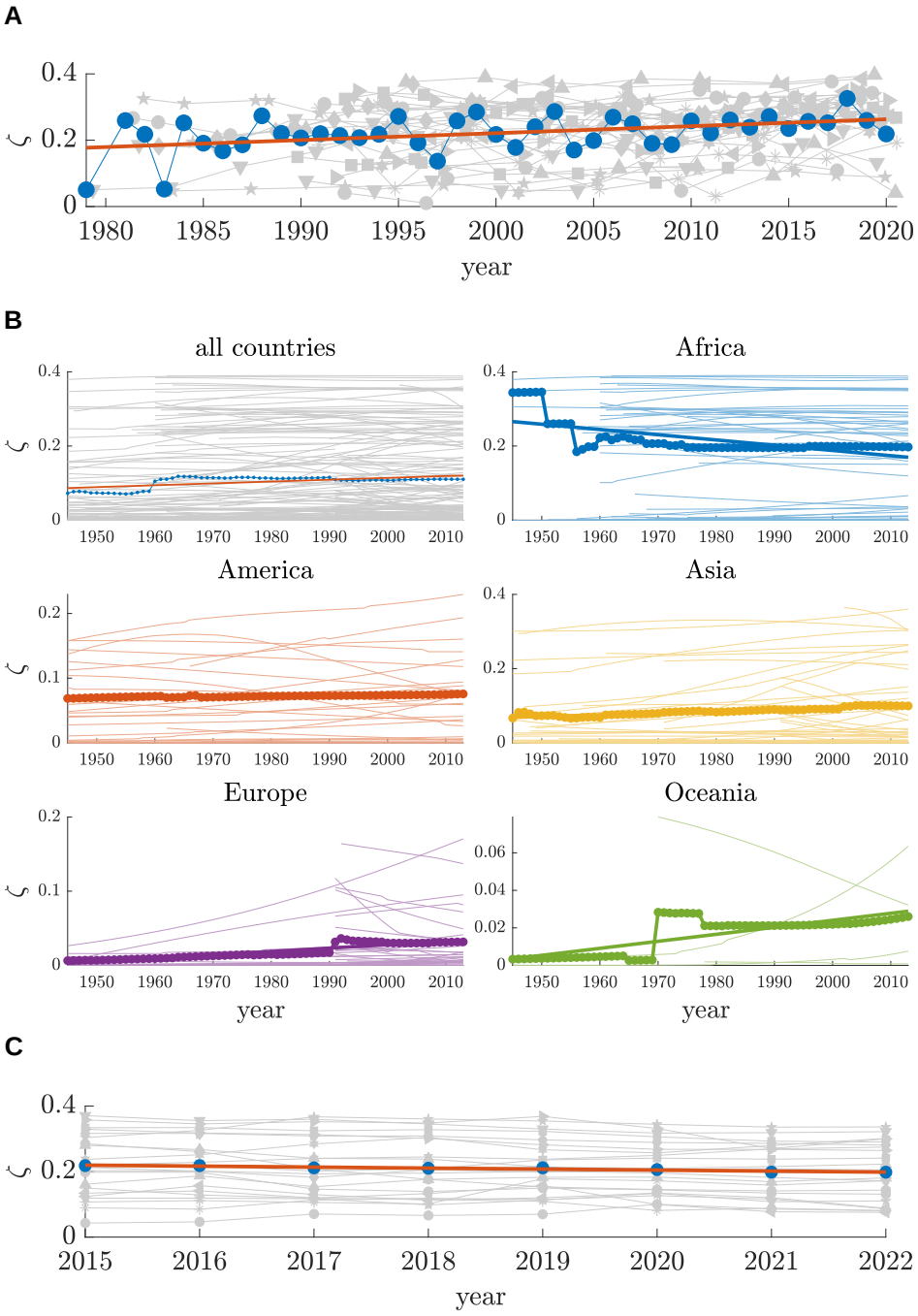

Fig. 5. Frustration over time in various applications. A) Parliamentary networks. B) Ethnolinguistic networks. C) Smartphone market shares. In panels A and C, the time course of frustration for the various countries is shown in gray. The yearly means is highlighted in blue and the linear fit in red. In panel B, the data are split across continents and the same quantities are shown. The discontinuities in the mean correspond essentially to new countries being added to (or removed from) the database.

$m = pn^2$, $\frac{c_i^2}{n^2} = \frac{pc_i^2}{m}$ is the amount of positive edges of the ith group over the total of edges; hence, $H = \sum_{i=1}^{q} \frac{c_i^2}{n^2} = \frac{p\sum_{i=1}^{q} c_i^2}{m}$ represents the fraction of positive edges. Consequently, $F = 1 - H$ represents the fraction of negative edges. The effective number of groups $E = \frac{1}{H} = \frac{m}{p\sum_{i=1}^{q} c_i^2}$ is an equivalent number of groups: it represents the number of equal-size groups which would have yield the same value of the Simpson index H (i.e. the same fraction of positive edges) as do the actual unequal groups (37). Such measure does not seem to have a classical interpretation in the theory of signed graphs. It might be of relevance when classifying weakly balanced signed networks, or in the inverse problem of community detection on signed graphs (38, 39).

For Erdös–Rényi networks, the relationships between the diversity indices and frustration are valid regardless of the group size distribution. In fact, heterogeneity in group size does not induce heterogeneity in edge degree distribution, but only in *signed* edge degree distribution, and both F and ζ capture such difference. When instead the edge distribution deviates from an Erdös–Rényi model, the formulae for ζ and F may deviate from each other. A simple enough case is when the probability of positive edges differs from that of negative edges, i.e. when the edge density in the

diagonal and off-diagonal blocks of A differs. As shown in Theorem 2 of the supplementary material, in this case the formulae for ζ, F, and H, including Eq. 5, hold with only minor corrections.

Several measures, alternative to frustration, have been proposed in the literature to quantify strong (and weak) unbalance, see e.g. Refs. (25, 27–29). They range from counting cycles, possibly discounting for cycle length, to computing eigenvalues of a signed Laplacian matrix associated to our matrix A (40). In the supplementary material, we consider three such measures, taken from Refs. (27, 28, 40), and compare them with ζ and F. No significant extra relationship between the diversity indices and these alternative "distance to balance" measures emerges from the analysis, see Fig. S20.

The formalism of signed graphs was first developed in the field of Social Psychology as a way to formalize heuristic concepts like "the enemy of my enemy is my friend" and similar triadic relationships (24, 41). In fact, in a large part of the literature, positive edges are still given some form of positive connotation (friendship between individuals, alliance between political actors, trust among communicating computer nodes, collaboration between businesses, etc.), while negative edges represent instead an antagonistic attitude (unfriendliness between individuals, rivalry between political actors, mistrust among computers, competition between businesses, etc.). In this work, instead, edge signs are primarily a way to distinguish the two categories that enter into a diversity index (within- and between-groups interactions), not necessarily redirecting to a friendly/unfriendly connotation. For the data we analyze, such connotation may or may not be present. For instance, for the parliamentary networks, we can reasonably assume that MPs of the same party collaborate with each other and are rival of the MPs of the other parties. For the smartphone market shares, an association between individuals based on their choice of smartphone brand is a rather weak and unsubstantial one, while it makes sense to consider negative edges as an expression of competition among smartphone brands in the aggregated network W.

If we think of frustration as "disorder" in a signed graph, then an increase of fragmentation in a population leads to an increase in the disorder encoded in the associated network. The consequences of an increased disorder are context-dependent and their interpretation may be sometimes controversial. For instance, we have shown in Ref. (33) that in the political arena an increased frustration reflects into an increased difficulty in the governance of a country, in particular into a longer negotiation phase in the government formation process that follows a general election. However, we notice that the opposite of high fractionalization (and of high frustration), that is, strong balance, corresponds to single party rule but also to two-party systems. The canonical example in this context is the US political system (42, 43), which, in spite of being strongly balanced, has its own problems when it comes to political governance even though it lacks disorder. On a similar tone, ethnolinguistic fragmentation has sometimes been associated to higher degree of conflict in a society, possibly leading to lack of social cohesion, prejudices, and to political and economical costs (7, 44). On the other hand, researchers have observed that ethnical heterogeneity has also benefits, e.g. diverse-thinking approaches can lead to an increased capacity for problem solving and may nurture economic growth (8, 45, 46). The fact that antitrust bodies forbid industrial sectors with high H (and hence with low F and low ζ) is another example that "disorder" may have virtuous effects.

The three classes of examples we present aim to highlight the different features of the weakly balanced structure in the graphs which we consider in the paper: nodes can be elements of the population (as for the parliamentary networks), but for extremely large populations (as in the ethnolinguistic networks), under an assumption of equiprobable edges, a compact representation, lumping together all elements of a group into a single node and rescaling the edge weights according to the group size, is readily available through the condensed matrix W. Such a representation is meaningful in a broader context, in which diversity indices are used and useful for the group-level condensed network but maybe not so much for the individual-level networks (as for the smartphone market shares).

A challenging problem ahead is to use some of the tools presented in this paper for community detection problems, in which a signed graph is given but not a group partition, in the style of Refs. (38, 39). We notice that the assumption made here of homogeneous edge degree distribution is used in the so-called constant Potts model approach (47, 48) to community detection, even though mostly for unsigned graphs. How to exploit diversity measures in this context for signed graphs is a problem that still needs to be explored.

Methods

Strong and weak balance for signed graphs

Consider an undirected signed graph $\mathcal{G} = \{\mathcal{V}, \mathcal{E}, A\}$, where $\mathcal{V} = \{1, \ldots, n\}$ is the node set, $\mathcal{E} = \mathcal{V} \times \mathcal{V}$ is the edge set, and A is an $n \times n$ symmetric signed adjacency matrix of elements $A_{ij} \in \{0, \pm 1\}$. We assume that each edge is equiprobable with probability p, and call $m = pn^2$ the (expected) number of edges.

A signed graph is said *strongly balanced* if there exists a partition of the nodes into two factions $\mathcal{F}^+$ and $\mathcal{F}^-$, with $\mathcal{F}^- \cup \mathcal{F}^+ = \mathcal{V}$ and $\mathcal{F}^- \cap \mathcal{F}^+ = \emptyset$, such that $i, j \in \mathcal{F}^+$ (or $i, j \in \mathcal{F}^-$) corresponds to $A_{ij} \geq 0$, while $i \in \mathcal{F}^-$ and $j \in \mathcal{F}^+$ corresponds to $A_{ij} \leq 0$.

The *frustration* of a signed graph $\mathcal{G}$ is defined as the least fraction of edges that must change sign in order to achieve strong balance. It can also be expressed as the minimum over all "spin" assignments $s_i = \pm 1$ of the "energy" functional $e(s) = \frac{1}{2m} \sum_{i,j \in \mathcal{E}} (1 - A_{ij} s_i s_j)$ as in Eq. 3. Notice that in matrix form $e(s) = \mathbb{1}^T (|A| - SAS)\mathbb{1}$, where $\mathbb{1} = [1 \ldots 1]^T \in \mathbb{R}^n$ is the vector of all 1, $S = \mathrm{diag}\{s_1, \ldots, s_n\}$ is a diagonal matrix of entries ± 1, and $|A| = \mathrm{abs}(\mathbf{A})$ (49). The matrix SAS is sometimes called a gauge transformation of A (26).

A signed graph is said *weakly balanced* if the adjacency matrix A has a block diagonal structure in which the $q > 1$ diagonal blocks have all nonnegative edges and the off-diagonal blocks have all nonpositive edges, see Fig. 1B. The q diagonal blocks correspond to groups of nodes which we denote $\mathcal{C}_1, \ldots, \mathcal{C}_q$, of dimension $c_1, \ldots, c_q$ such that $\sum_{i=1}^q c_i = n$, $\mathcal{C}_i \cap \mathcal{C}_j = \emptyset$, $\bigcup_{i=1}^q \mathcal{C}_i = \mathcal{V}$.

For block partitioned weakly balanced matrices, it is possible to "condensate" each block into a single node, obtaining the $q \times q$ signed weighted adjacency matrix

$$W = p \begin{bmatrix} c_1^2 & -c_1 c_2 & \ldots & -c_1 c_q \\ -c_1 c_2 & c_2^2 & & \\ \vdots & & \ddots & \\ -c_1 c_q & & & c_q^2 \end{bmatrix}. \tag{7}$$

As shown in the supplementary material, this allows to reexpress frustration in term of W as

$$\zeta = \frac{1}{2m} \min_{S_q = \mathrm{diag}\{s_1, \ldots, s_q\}_{s_i = \pm 1}} \mathbb{1}_q^T (|W| - S_q W S_q) \mathbb{1}_q, \tag{8}$$

where $\mathbb{1}_q \in \mathbb{R}^q$ and $S_q = \mathrm{diag}\{s_1, \ldots, s_q\}$ is a $q \times q$ diagonal matrix of ± 1 (one for each block). That is to say, the minimum of the energy functional $e(s)$ corresponds to an equal-size (or as equal as possible) splitting of the groups into the two factions $\mathcal{F}^-$ and $\mathcal{F}^+$,

and computing ζ reduces to computing such optimal group partition of $\mathcal{C}_1, \ldots, \mathcal{C}_q$, denoted $\{\mathcal{F}^+_{\text{best}}, \mathcal{F}^-_{\text{best}}\}$. Direct computations (see Theorem 1 in the supplementary material) show that

$$\zeta = \frac{p}{m} \min_{\mathcal{F}^+} \left(\sum_{\substack{i,j \in \mathcal{F}^+ \\ i \neq j}} c_i c_j + \sum_{\substack{i,j \in \mathcal{F}^- \\ i \neq j}} c_i c_j \right), \tag{9}$$

i.e. what is minimized is the total amount of edges in the off-diagonal subblocks on each side of the partition, see Fig. 1 for an interpretation.

Fractionalization and other diversity indices

Given a population of n elements, split into q groups of cardinality $c_1, \ldots, c_q$, the *fractionalization index* F (also known as the Gini–Simpson index, or Blau index, or Gibbs–Martin index) is given by Eq. 1. Associated to F are the *effective number of groups* E (also known as the Laakso–Taagepera effective number of parties or the inverse Simpson index), defined as in Eq. 2, and the Simpson index (also known as the Herfindahl–Hirschman index) $H = \frac{1}{E} = 1 - F$.

Fractionalization and weakly balanced signed networks

There is a natural way to associate a splitting of a population into q groups with a weakly balanced signed network, and it consists in associating each group with a block in a signed block matrix A as the one described above. F, which represents the probability that two entities from the population do not belong to the same group, corresponds in this representation to the fraction of negative edges of A, see Fig. 1C, while H (probability of within-group encounters) becomes the fraction of positive edges of A.

Frustration and fractionalization

Letting $n_{\mathcal{F}^+}$ and $n_{\mathcal{F}^-}$ be the cardinalities of the $\mathcal{F}^+$ and $\mathcal{F}^-$ factions, $n_{\mathcal{F}^+} + n_{\mathcal{F}^-} = n$, then it is also (see Theorem 1 in the supplementary material)

$$\zeta = F - \frac{2}{n^2} \max_{\mathcal{F}^+} \left(n_{\mathcal{F}^+} (n - n_{\mathcal{F}^+}) \right). \tag{10}$$

The maximum in this expression is obtained when $n_{\mathcal{F}^+} = n - n_{\mathcal{F}^+}$ if possible, i.e. when the optimal partition of the maximization in Eq. 4, $\mathcal{F}^+_{\text{best}}, \mathcal{F}^-_{\text{best}}$, has cardinality $n_{\mathcal{F}^+_{\text{best}}} = n_{\mathcal{F}^-_{\text{best}}} = n/2$. When such a partition into equally sized factions exists, then it is $\zeta = F - 1/2$. In all other cases, one of the two optimal factions $\mathcal{F}^+_{\text{best}}, \mathcal{F}^-_{\text{best}}$ (say $\mathcal{F}^+_{\text{best}}$) will be larger than the other. Letting $n_{\mathcal{F}^+_{\text{best}}} = \frac{n}{2} + \ell_{\text{best}}$, where ℓ_{best} is the node excess in the best bipartition of $\mathcal{C}_1, \ldots, \mathcal{C}_q$, then we get the relationship in Eq. 5 between ζ and F, i.e. the frustration is directly proportional to the fractionalization up to the correction factor $r_{\text{best}} = \frac{\ell_{\text{best}}}{n/2}$, see Theorem 1 in the supplementary material.

As we vary q and n, $F \in [0, 1 - \frac{1}{n}]$ and $\zeta \in [0, 1/2]$. When $q = 1$ then $F = 0$ and $\zeta = 0$, since $\ell_{\text{best}} = n/2$. When $q = 2$ then the graph is always strongly balanced (i.e. $\zeta = 0$) but $F \neq 0$. When $q = n$ (i.e. all groups have dimension 1), then

$$\ell_{\text{best}} = \begin{cases} 0 & \text{if } n \text{ even} \\ 1 & \text{if } n \text{ odd} \end{cases}$$

and $F = 1 - 1/n$, meaning that

$$\zeta = \begin{cases} 1/2 - 1/n & \text{if } n \text{ odd} \\ 1/2 - (n-2)/n^2 & \text{if } n \text{ even} \end{cases}$$

and $\lim_{n \to \infty} \zeta = 1/2$. It can be shown that ζ is always upper bounded by 1/2.

Invariance to edge density

For Erdös–Rényi weakly balanced signed graphs (i.e. graphs in which each edge appears with a probability $0 < p \leq 1$, and in which the sign pattern is that of a weakly balance graph), the definition of F, H, and E is invariant to edge density. In fact, for any edge probability p, from $m = pn^2$, $H = \frac{\sum_{i=1}^q pc_i^2}{pn^2} = \frac{\sum_{i=1}^q c_i^2}{n^2}$, and similarly for F and E. As can be deduced from Eq. 9, also ζ is invariant to p (recall that ζ is defined as the *fraction* of edges that must change sign to get strong balance). As we vary p, also the least number of edges that must flip sign to achieve strong balance must be rescaled according to p, but the fraction of such edges over the total is unchanged, hence so is the frustration ζ.

Computing frustration for weakly balanced Erdös–Rényi networks

The expression in Eq. 10 attains its minimum when $\mathcal{C}_1, \ldots, \mathcal{C}_q$ are partitioned into two factions of equal, or as equal as possible, size. Hence, the computation of ζ reduces to the calculation of $\mathcal{F}^+_{\text{best}}, \mathcal{F}^-_{\text{best}}$ that solve Eq. 4. Such a problem is computationally much more efficient than solving Eq. 3. The number of possible combinations still grows exponentially as 2^{q-1}, but for moderate sizes the minimum can be computed exactly, while for large q heuristics can be found. These algorithms are particularly effective when the number of groups is sufficiently high (since $\sum_{i=1}^q c_i = n$, q large means that many groups of relatively small size must exist for a given n). The "ground state" is typically degenerate in these cases, i.e. many optimal partitions $\mathcal{F}^+_{\text{best}}, \mathcal{F}^-_{\text{best}}$ exist, all corresponding to the same ζ.

Notes

[a] H is also the contraharmonic mean of the proportional abundances $\frac{c_i}{n}$. As such, it can be considered the sum of the arithmetic mean and the variance of the $\frac{c_i}{n}$ divided by their arithmetic mean, see Refs. (35, 36).

[b] Since p is a probability, m is the expected number of edges. The adjective "expected" is disregarded thereafter. On a similar tone, to reduce bookkeeping, edges are counted twice and self-loops (i.e. diagonal elements A_{ii}) are also counted when present, meaning that when $p = 1$, $m = n^2$. When edges are counted with a precise formula ($m = p\frac{n^2+n}{2}$ if $A_{ii} = 1$ for all i, $m = p\frac{n^2-n}{2}$ when $A_{ii} = 0$ for all i), then an additional constant may appear in ζ in Eq. 3 and in the relation of Eq. 5. Since $e(s)$ and ζ are always defined up to an additive constant (26), this factor can be disregarded for simplicity of exposition.

Supplementary Material

Supplementary material is available at *PNAS Nexus* online.

Funding

This work was supported in part by grants from the Swedish Research Council (grant no. 2020-03701 to C.A.) and by the ELLIIT framework program at Linköping University.

Author Contributions

C.A. designed research and wrote the paper. A.F., M.R., and C.A. performed research and analyzed data. A.F. and C.A. contributed new analytical tools.

Data Availability

All data are publicly available (parliamentary networks: supplementary material of Ref. (33); ethnolinguistic networks: downloaded from Ref. (34); smartphone market shares: downloaded from https://gs.statcounter.com/vendor-market-share). The data and code used in this study are available at https://zenodo.org/records/10479515.

References

1 Hill MO. 1973. Diversity and evenness: a unifying notation and its consequences. *Ecology*. 54(2):427–432.
2 Heip CHR, Herman PMJ, Soetaert K. 1998. Indices of diversity and evenness. *Oceanis*. 24(4):61–88.
3 Solanas A, Selvam RM, Navarro J, Leiva D. 2012. Some common indices of group diversity: upper boundaries. *Psychol Rep*. 111(3):777–796.
4 Solow AR, Polasky S. 1994. Measuring biological diversity. *Environ Ecol Stat*. 1:95–103.
5 Lieberson S. 1969. Measuring population diversity. *Am Sociol Rev*. 34(6):850–862.
6 Xu S, Böttcher L, Chou T. 2020. Diversity in biology: definitions, quantification and models. *Phys Biol*. 17(3):031001.
7 Alesina A, Devleeschauwer A, Easterly W, Kurlat S, Wacziarg R. 2003. Fractionalization. *J Econ Growth*. 8:155–194.
8 Pelled LH. 1996. Demographic diversity, conflict, and work group outcomes: an intervening process theory. *Organ Sci*. 7(6):615–631.
9 Laakso M, Taagepera R. 1979. "Effective" number of parties: a measure with application to West Europe. *Comp Polit Stud*. 12(1):3–27.
10 Rae DW, Taylor M. 1970. *The analysis of political cleavages*. New Haven (CT): Yale University Press.
11 Simpson EH. 1949. Measurement of diversity. *Nature*. 163(4148):688.
12 Blau PM. 1977. *Inequality and heterogeneity: a primitive theory of social structure*. Vol. 7. New York (NY): Free Press.
13 Gibbs JP, Martin WT. 1962. Urbanization, technology, and the division of labor: international patterns. *Am Sociol Rev*. 27:667–677.
14 Hirschman AO. 1964. The paternity of an index. *Am Econ Rev*. 54(5):761–762.
15 US Department of Justice and the Federal Trade Commission. 2010. Horizontal merger guidelines. Par. 5.3. https://www.justice.gov/atr/horizontal-merger-guidelines-08192010#5c.
16 Wasserman S, Faust K. 1994. *Social network analysis: methods and applications*. Structural analysis in the social sciences. Cambridge: Cambridge University Press.
17 Mezard M, Parisi G, Virasoro M. 1986. *Spin glass theory and beyond*. Singapore: World Scientific.
18 Iacono G, Ramezani F, Soranzo N, Altafini C. 2010. Determining the distance to monotonicity of a biological network: a graph-theoretical approach. *IET Syst Biol*. 4(3):223–235.
19 Altafini C. 2013. Consensus problems on networks with antagonistic interactions. *IEEE Trans Autom Control*. 58(4):935–946.
20 Aref S, Wilson MC. 2019. Balance and frustration in signed networks. *J Complex Netw*. 7(2):163–189.
21 Traag V, Doreian P, Mrvar A. 2019. Partitioning signed networks. In: Doreian P, Batagelj V, Ferligoj A, editors. *Advances in network clustering and blockmodeling*. New York (NY): Wiley. p. 225–249.
22 Zaslavsky T. 1982. Signed graphs. *Discrete Appl Math*. 4(1):47–74.
23 Davis JA. 1967. Clustering and structural balance in graphs. *Hum Relat*. 20:181–187.
24 Cartwright D, Harary F. 1956. Structural balance: a generalization of Heider's theory. *Psychol Rev*. 63:277–292.
25 Aref S, Wilson MC. 2018. Measuring partial balance in signed networks. *J Complex Netw*. 6(4):566–595.
26 Facchetti G, Iacono G, Altafini C. 2011. Computing global structural balance in large-scale signed social networks. *Proc Natl Acad Sci U S A*. 108:20953–20958.
27 Estrada E, Benzi M. 2014. Walk-based measure of balance in signed networks: detecting lack of balance in social networks. *Phys Rev E*. 90(4):042802.
28 Kirkley A, Cantwell GT, Newman MEJ. 2019. Balance in signed networks. *Phys Rev E*. 99(1):012320.
29 Singh R, Adhikari B. 2017. Measuring the balance of signed networks and its application to sign prediction. *J Stat Mech Theory Exp*. 2017(6):063302.
30 Fontan A, Altafini C. 2021. The role of frustration in collective decision-making dynamical processes on multiagent signed networks. *IEEE Trans Autom Control*. 67(10):5191–5206.
31 Harary F. 1959. On the measurement of structural balance. *Behav Sci*. 4(4):316–323.
32 Barahona F. 1982. On the computational complexity of Ising spin glass models. *J Phys A: Math Gen*. 15(10):3241–3253.
33 Fontan A, Altafini C. 2021. A signed network perspective on the government formation process in parliamentary democracies. *Sci Rep*. 11(1):5134.
34 Dražanová L. 2020. Introducing the historical index of ethnic fractionalization (HIEF) dataset: accounting for longitudinal changes in ethnic diversity. *J Open Humanit Data*. 6(1):1–8.
35 Feld SL, Grofman B. 2007. The Laakso–Taagepera index in a mean and variance framework. *J Theor Polit*. 19(1):101–106.
36 Caulier J-F. 2011. The interpretation of the Laakso–Taagepera effective number of parties. https://shs.hal.science/halshs-00565315.
37 Taagepera R, Grofman B. 1981. Effective size and number of components. *Sociol Methods Res*. 10(1):63–81.
38 Traag VA, Bruggeman J. 2009. Community detection in networks with positive and negative links. *Phys Rev E*. 80(3):036115.
39 Esmailian P, Jalili M. 2015. Community detection in signed networks: the role of negative ties in different scales. *Sci Rep*. 5(1):14339.
40 Kunegis J. 2014. Applications of structural balance in signed social networks, arXiv, arXiv:1402.6865, preprint: not peer reviewed.
41 Heider F. 1946. Attitudes and cognitive organization. *J Psychol*. 21:107–122.
42 Andris C, *et al.* 2015. The rise of partisanship and super-cooperators in the US house of representatives. *PLoS One*. 10(4):e0123507.
43 Aref S, Neal ZP. 2021. Identifying hidden coalitions in the US house of representatives by optimally partitioning signed networks based on generalized balance. *Sci Rep*. 11(1):19939.
44 Annett A. 2001. Social fractionalization, political instability, and the size of government. *IMF Staff Papers*. 48(3):561–592.
45 Alesina A, La Ferrara E. 2005. Ethnic diversity and economic performance. *J Econ Lit*. 43(3):762–800.
46 Peng Z, Madni GR, Anwar MA, Yasin I. 2023. Imperative of institutions for effective relationship between economic

performance and ethnic diversity. *J Knowl Econ*. https://doi.org/10.1007/s13132-023-01195-y.
47 Traag VA, Van Dooren P, Nesterov Y. 2011. Narrow scope for resolution-limit-free community detection. *Phys Rev E*. 84(1):016114.
48 Traag VA, Waltman L, Jan Van Eck N. 2019. From Louvain to Leiden: guaranteeing well-connected communities. *Sci Rep*. 9(1):5233.
49 Shi G, Altafini C, Baras JS. 2019. Dynamics over signed networks. *SIAM Rev*. 61(2):229–257.